J. Fluid Mech. (1978), *vol.* 89, *part* 1, *pp.* 173–190
Printed in Great Britain

A theoretical and experimental study of thermal disturbances propagating in a fluid layer heated from below

By B. M. BERKOVSKY, V. E. FERTMAN, A. K. SINITSYN AND YU. I. BARKOV

The Luikov Heat and Mass Transfer Institute, Academy of Sciences of the Byelorussian SSR, Minsk, U.S.S.R.

(Received 4 August 1976 and in revised form 13 June 1978)

A theoretical and experimental study is presented of the longitudinal propagation of disturbances in an unstably stratified fluid layer, especially those generated by periodic temperature fluctuations at a side boundary. The most important characteristics of the waves at both supercritical Rayleigh numbers, in the presence of steady roll-like cells, and subcritical Rayleigh numbers are determined.

1. Introduction

Wave propagation of interrelated thermal and hydrodynamic (thermoconvective) disturbances is a simplified example of the complex thermoconvective processes in non-isentropic fluids being investigated in meteorology and oceanography.

It is a known fact that in the case of an unstably stratified fluid layer the hydrodynamic equations in the classical approximation of an ideal fluid do not allow wave solutions. Luikov & Berkovsky (1969*a*, 1970) were the first to point out the existence of weakly damped waves in an unstably stratified layer of a viscous heat-conducting fluid (i.e. $\lambda/L \ll 1$, where λ is the wavelength and L is the damping length), and called these waves thermoconvective waves (TCW). The existence of TCW has been confirmed experimentally (Barkov, Berkovsky & Fertman 1974). The characteristics of TCW in fluids with peculiar properties (i.e. viscoelastic, ferromagnetic or electrically conducting fluids) in both a gravity force field and magnetic and electric fields have been investigated by a number of authors (Luikov & Berkovsky 1969*b*; Gupta & Gupta 1973; Berkovsky, Bashtovoi & Lipkina 1970; Takashima 1972*a*, *b*). In all this work TCW have been studied theoretically by employing idealized one-dimensional mathematical models in which the effects of boundaries and convective motion in the layer are ignored.

The corresponding problem of the propagation of internal gravity waves (IGW) in a stably stratified fluid, where viscosity and heat conduction are taken into account, has been studied by LeBlond (1966), Golitsin (1965), Gershuni & Zhukhovitsky (1972), Giterman & Shteinberg (1972), Thomas & Stevenson (1973) and Sinitsyn & Fertman (1976).

Thus thermoconvective disturbances may propagate either as IGW (stably stratified fluid) or as TCW (unstably stratified fluid). Although TCW and IGW are described by the same equations, they have a different physical nature. While a necessary condition

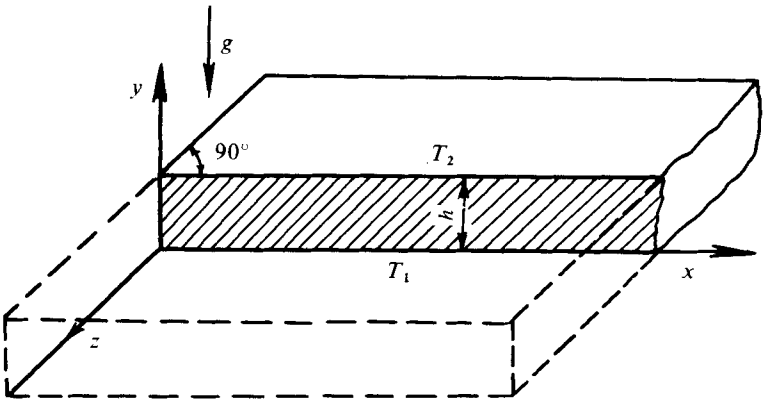

FIGURE 1. Section of the horizontal fluid layer.

for the propagation of IGW is the presence of a restoring force (stably stratified fluid), viscosity and heat conduction leading only to damping of the waves, for the propagation of TCW the simultaneous effect of viscosity and heat conduction in the case of an unstably stratified fluid is of primary importance.

A thorough investigation of the mechanism of propagating TCW and their main characteristics will help to clarify the development of unsteady-state flows in a non-isothermal fluid.

In accordance with the problem stated, an analysis is carried out of the linearized problem of the propagation of small amplitude waves in a layer with free boundaries. This allows determination of a region with TCW, their spectral composition and their main characteristics (§ 3). Numerical calculation by a network method allowing for nonlinear effects reveals the mechanism of TCW propagation in the presence of steady convection cells in the layer (§ 4). In § 5 a set-up for laboratory experiments on TCW propagation is described.

2. Statement of the problem

A plane horizontal layer of thickness h is considered. The upper and lower boundaries of the layer are maintained at temperatures T_1 and T_2, respectively. The solution to the problem is sought in a plane finite region which is a vertical cross-section of the layer (figure 1), the region's length being l. External disturbances are introduced at the vertical boundary at $x = 0$ and are assumed to be periodic oscillations in the temperature. Let us consider the propagation of these disturbances through the layer in the x direction. The mathematical formulation of the problem is based on the ordinary equations of natural convection in the Boussinesq approximation. In dimensionless form the equations may be written in terms of the stream function ψ, the vorticity ϕ and the temperature Θ as

$$\frac{\partial \phi}{\partial t} = \frac{\partial}{\partial x}\left(\frac{\partial \phi}{\partial x} - u\phi\right) - \frac{\partial}{\partial y}\left(\frac{\partial \phi}{\partial y} - v\phi\right) + Gr\frac{\partial \Theta}{\partial x}, \tag{1}$$

$$\frac{\partial \Theta}{\partial t} = \frac{\partial}{\partial x}\left(\frac{1}{Pr}\frac{\partial \Theta}{\partial x} - u\Theta\right) + \frac{\partial}{\partial y}\left(\frac{1}{Pr}\frac{\partial \Theta}{\partial y} - v\Theta\right), \tag{2}$$

$$\nabla^2\psi = -\phi, \quad u = \partial\psi/\partial y, \quad v = -\partial\psi/\partial x. \tag{3}$$

The boundary conditions for the temperature are

$$\left.\begin{aligned} \Theta|_{y=0} = \alpha, \quad \Theta|_{y=1} = 0, \quad \Theta|_{x=l/h} = \alpha(1-y), \\ \Theta|_{x=0} = \alpha(1-y) + \tfrac{1}{2}(1-|\alpha|)\sin \pi y \sin \omega t. \end{aligned}\right\} \tag{4}$$

Two types of boundary conditions for the velocity are used.

(*a*) Rigid horizontal boundaries:

$$\psi|_{y=0,1} = [\partial\psi/\partial y]_{y=0,1} = 0. \tag{5}$$

(*b*) Free horizontal boundaries:

$$\psi|_{y=0,1} = [\partial^2\psi/\partial y^2]_{y=0,1} = 0. \tag{6}$$

Here $Gr = \beta g h^3(A_0 + |\gamma h|)/\nu^2$, a Grashof number; $Pr = \nu/a$, a Prandtl number; $\alpha = \gamma h/(A_0 + |\gamma h|)$, a dimensionless parameter which characterizes the ratio between the amplitude A_0 of the temperature oscillations at the boundaries and the vertical temperature drop in the layer γh; $0 \leqslant \alpha \leqslant 1$; γ is the constant vertical temperature gradient; ν is the fluid viscosity; a is the thermal diffusivity; $\beta = -\rho^{-1}\partial\rho/\partial T$, a thermal expansion coefficient; g is the gravitational acceleration; ω is the frequency; ρ is the fluid density. The following quantities are chosen as characteristic values: h for distances, ν/h for velocities, h^2/ν for times and $A_0 + |\gamma h|$ for temperatures.

Along with (1)–(3), the linearized system which governs the propagation of small amplitude waves is considered:

$$\frac{\partial \nabla^2\psi}{\partial t} = \nabla^2\nabla^2\psi - Gr\frac{\partial \Theta}{\partial x}, \tag{7}$$

$$\frac{\partial \Theta}{\partial t} = \frac{1}{Pr}\nabla^2\Theta - \alpha\frac{\partial \psi}{\partial x}. \tag{8}$$

In this case the boundary conditions for Θ are written as

$$\Theta|_{y=0,1} = \Theta|_{x=l/h} = 0, \quad \Theta|_{x=0} = \tfrac{1}{2}(1-|\alpha|)\sin \pi y \sin \omega t. \tag{9}$$

Equations (7) and (8) are obtained from (1)–(4) by substituting the solution $\Theta = \alpha(1-y) + \Theta'$, $\psi = \psi'$ and neglecting terms of second order. Here Θ' and ψ' are small disturbances and we have dropped the primes. Estimates have shown that the linear approximation (7) and (8) is valid for both subcritical and small supercritical Rayleigh numbers when the intensity of convective motion is not great.

The choice of the dependence $\sin \pi y$ in the boundary conditions (4) and (9) is explained by the fact that this mode corresponds to the smallest decrease in perturbation damping.

3. Propagation of small amplitude thermoconvective disturbances through a layer with free boundaries

For a qualitative analysis of wave propagation of thermoconvective disturbances, we shall consider small wave amplitudes and low rates of motion in a layer when the linear approximation (7) and (8) is valid. With the boundary condition (6), the problem may be solved analytically. Consider a semi-infinite layer ($l \to \infty$).

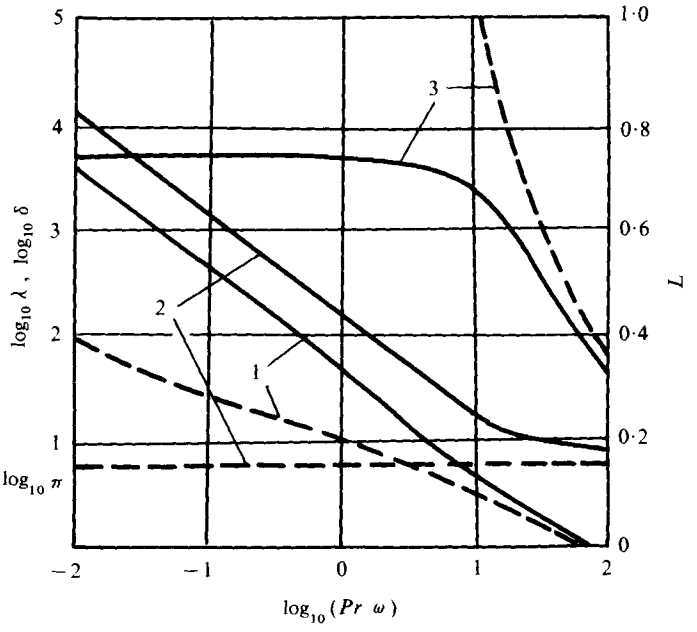

FIGURE 2. Characteristics of temperature waves in an isothermal fluid layer. (1) λ. (2) δ. (3) L. ——, characteristics of a one-dimensional wave.

In the case of an isothermal layer ($T_1 = T_2$, $\alpha = 0$) the temperature equation (8) is independent of the velocity since the convective terms are of second order. An exact solution has been obtained for a temperature wave excited by periodic temperature oscillations of the vertical boundary and also for the convective motion which arises in the layer. An analysis of the solution obtained has revealed that the isothermal boundaries of the layer essentially affect the characteristics of the temperature wave compared with the one-dimensional problem (Carslaw & Jaeger 1964, p. 70): the logarithmic decrement $\delta_x = 2\pi \operatorname{Im} K/\operatorname{Re} K$ and the wavelength $\lambda = 2\pi/\operatorname{Re} K$ are increased (K = wavenumber). The damping length of the wave $L = \ln 10/\operatorname{Im} K$, the distance over which the waves propagate, will be determined as the distance x at which the amplitude of the disturbances propagating through the layer becomes less than one-tenth of the amplitude at the vertical boundary. Then the damping length is always smaller than three-quarters of the thickness of the layer (figure 2). In fact, this is a periodic rather than a wave process. Convective motion is localized near a side boundary as a single convective cell, which periodically changes its direction with the frequency of the temperature oscillations at the side boundary. At a distance of $x = 1{\cdot}5h$ the velocity and temperature amplitudes attenuate in approximately in 100 periods.

For a layer with a vertical temperature gradient equations (7) and (8) are coupled. In this case the solution to the problem is sought as a plane wave

$$\{\Theta, \psi\} = \{\Theta_0, \phi_0\} \sin \pi y \exp[i(\omega t - Kx)]. \tag{10}$$

The dispersion equation is a bicubic polynomial with respect to the wavenumber K (Chandrasekhar 1961, p. 24):

$$(iPr\omega + K^2 + \pi^2)(i\omega + K^2 + \pi^2)(K^2 + \pi^2) - K^2 Ra = 0, \tag{11}$$

where $Ra = GrPr\alpha$ is the Rayleigh number. The frequency ω is assumed to be a specified real quantity equal to the frequency of the temperature oscillations at the side boundary $x = 0$. Three of the roots of (11), K_1, K_2 and K_3, say, are consistent with the condition for attenuation of the waves at infinity ($\mathrm{Im}\, K_j < 0$). The excited wave may thus be expressed as a superposition of three harmonics:

$$\left.\begin{aligned} \Theta = \sin \pi y \,\mathrm{Im} \sum_{j=1}^{3} c_j \exp\left[i(\omega t - K_j x)\right], \quad \phi = \sin \pi y \,.\, \mathrm{Im} \sum_{j=1}^{3} c_j \psi_{0j} \exp\left[i(\omega t - K_j x)\right], \\ \psi_{0j} = \left[i\omega + (K_j^2 + \pi^2)/Pr\right]/iK_j\alpha. \end{aligned}\right\} \quad (12)$$

The complex coefficients c_j describe the energy which is spent on the excitation of each of the harmonics. They are found from the conditions at the vertical boundary, which give

$$\sum_{j=1}^{3} c_j = 1 - |\alpha|, \quad \sum_{j=1}^{3} \psi_{0j} c_j = 0, \quad \sum_{j=1}^{3} K_j \psi_{0j} c_j = 0. \quad (13)$$

The roots of the polynomial, the characteristics of the waves and the coefficients c_j have been calculated on a computer.

It should be noted that in the case of finite l all six roots of (11) are used to build up the solution and the expansion (12) contains six unknown coefficients. Additional equations for the three extra coefficients are found from the conditions at the boundary (Drazin 1975).

In the case of stable stratification (heating from above, $\alpha < 0$, $Ra < 0$) the amplitudes of two of the harmonics in (12) are damped by a factor of more than 500 in a distance of the order of the thickness ($L \ll h$) at any Ra, Pr and ω. Under the conditions given below the third harmonic is weakly damped compared with the other two. It penetrates to a greater depth and has a small decrement $\delta_x \ll 1$.

Thus in the range $x > h$ the wave (12) is described by one weakly damped harmonic and is represented by an internal gravity wave in a viscous heat-conducting fluid. In the limit of vanishing viscosity and heat conduction this wave turns into an undamped IGW in an ideal fluid layer. In order to study the dependence of the properties of the IGW on the oscillation frequency at the boundary, the roots of dispersion equation (13) have been calculated. The parabolic method was used to find all the complex roots of the polynomial. The relative error amounts to 1 %. The calculations were performed in a frequency range $1 \leqslant \omega \leqslant 10^3$ with a uniform logarithmic network. As is shown by calculations with viscosity and heat conduction taken into account, there is an 'optimal' oscillation frequency ω^* for the range of Ra and Pr considered, at which IGW are excited with a minimal logarithmic decrement. An analysis of the numerical results indicates that this optimal frequency is approximately equal to half the Brunt–Väisälä frequency: $\omega^* \simeq 0{\cdot}5(|Ra|/Pr)^{\frac{1}{2}}$. The optimal frequency is determined approximately from a plot of $\delta(\omega)$ and the uncertainty in its determination is therefore about 10 % since no special search for the minimum has been performed. The wavelength for the optimal frequency is about $3{\cdot}75h$ and does not depend on Ra and Pr.† The minimal decrement of IGW decreases as the absolute Rayleigh number grows (figure 3). As has been demonstrated by an analysis of the coefficients c_j, the energy associated with a weakly damped wave is within 15 % of the total energy of generation, the remaining portion being spent on excitation of two strongly damped harmonics. Thus, in a stably

† An asymptotic analysis of (13) carried out by Dr P. G. Daniels (private communication) has shown that, in fact, $\omega^* \sim (|Ra|/5Pr)^{\frac{1}{2}}$ and $\lambda \sim 4h$ as $|Ra| \to \infty$.

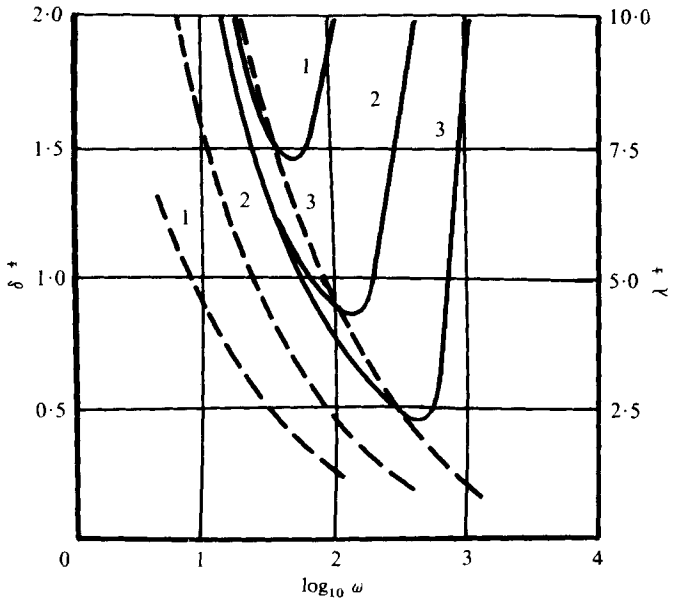

FIGURE 3. IGW characteristics in a layer with free boundaries. ---, λ. ——, δ. $Pr = 1$. (1) $Ra = 10^4$. (2) $Ra = 10^5$. (3) $Ra = 10^6$.

stratified layer, an internal weakly damped gravity wave propagates over the range of rather large negative Rayleigh numbers $Ra \leqslant -10^5$ if the frequency of the source is close to half the Brunt–Väisälä frequency.

Basically different waves propagate in an unstably stratified layer (heating from below, $\alpha > 0$, $Ra > 0$). Contrary to IGW, viscosity and heat conduction must be taken into account in their description and a force restoring a fluid particle to equilibrium is absent. An analysis of the roots of the dispersion equation (11) has revealed that in the wave (12) one harmonic is always damped by a factor of more than 1000 at a distance smaller than the layer thickness h, the two others penetrating to a large depth ($L \gg h$) and having a small decrement at Rayleigh numbers close to the critical value R^* which corresponds to the onset of mechanical instability of a horizontal fluid layer ($R^* = 657$ for a layer with free boundaries). To summarize, in the case of unstable stratification weakly damped waves, called thermoconvective waves, propagate. It is found that the region of weak attenuation of TCW is determined by critical or supercritical Rayleigh numbers ($Ra \geqslant R^*$) and small frequencies ($\omega < 10^{-1}$). The logarithmic decrement of TCW at such frequencies changes sharply near the boundary of stable mechanical equilibrium. The superposition of the two weakly damped harmonics at $x > h$ is recognized as a complex travelling wave with a sinusoidal amplitude:

$$\left.\begin{aligned} &\Theta = 0{\cdot}65(1-|\alpha|)\exp[\operatorname{Im} K_1 x]\sin\pi y\,\sin(\omega t - l_1 x)\,\sin(l_2 x - \xi),\\ &l_1 = \tfrac{1}{2}(\operatorname{Re} K_1 + \operatorname{Re} K_2),\quad l_2 = \tfrac{1}{2}(\operatorname{Re} K_1 - \operatorname{Re} K_2),\quad \xi = \text{constant}. \end{aligned}\right\} \tag{14}$$

Here K_1 and K_2 are the wavenumbers of the weakly damped harmonics in (12); $\operatorname{Im} K_1 = \operatorname{Im} K_2$. The most important characteristics of the wave are presented in figure 4. The wavelength $\lambda = 2\pi/l_1$ is of the order of $10h$ or larger. The periodicity of the amplitude may be attributed to periodic convective motion over the layer with period of the order of the layer thickness (curve 5).

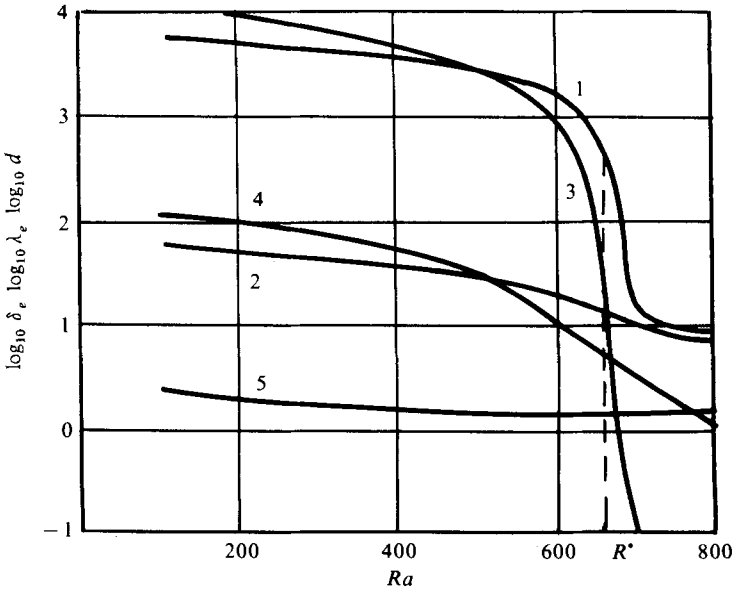

FIGURE 4. TCW characteristics in a layer with free boundaries. $Pr = 1{\cdot}0$. (1), (2) Wavelength $\lambda = 2\pi/l_1$ with $\omega = 0{\cdot}01$, 1. (3), (4) Damping decrement $\delta = 2\pi \operatorname{Im} K_1/l_1$ with $\omega = 0{\cdot}01$, 1. (5) Amplitude period $d = \pi/l_2$.

4. Propagation of thermoconvective disturbances of finite amplitude

An analysis of the above solutions of the linearized problem has demonstrated that the effect of weak damping of TCW should be most pronounced for supercritical Rayleigh numbers $Ra > R^*$, for which a linear approximation does not hold. A numerical simulation on a computer has been made in order to investigate theoretically TCW in a layer at supercritical Rayleigh numbers. The calculations have been performed by the network method under the boundary conditions (5). The network region was taken as a long rectangle ($l/h = 5$–15) to eliminate the effect of the rear wall. Equations (1)–(3) were approximated by a system of finite-difference equations. A monotonic conservative scheme of variable directions with second-order of accuracy with an automatic choice of a time step was employed (Nogotov & Sinitsyn 1975). The calculations were made on a uniform network with steps $\Delta x = \Delta y = \frac{1}{15}$ till the onset of steady periodic oscillations, after which the wave characteristics were taken. The phase characteristics of the waves were found from the propagation rate of a maximal temperature disturbance along the layer. An amplitude curve of the wave is calculated from

$$A_\Theta(x) = \max \Theta(x, 0{\cdot}5, t) - \min \Theta(x, 0{\cdot}5, t), \quad t \in [t_1, t_1 + 2\pi/\omega].$$

The Rayleigh number range considered ($0 \leqslant Ra \leqslant 10^5$) covers the propagation of TCW both against the background of a layer in mechanical equilibrium and in the presence of natural convection. The Prandtl number was taken to be equal to unity and the dimensionless frequency ω ranged between 0·5 and 10. This frequency range was chosen because calculations for small ω ($\omega < 0{\cdot}1$), where the effect of weak damping of TCW is expected, require much computer time. Oscillation amplitudes of the source $A_0 = |\gamma h|$, $\frac{1}{2}|\gamma h|$ and $\frac{1}{4}|\gamma h|$, corresponding to $\alpha = \frac{1}{2}$, $\frac{2}{3}$ and $\frac{4}{5}$, were considered.

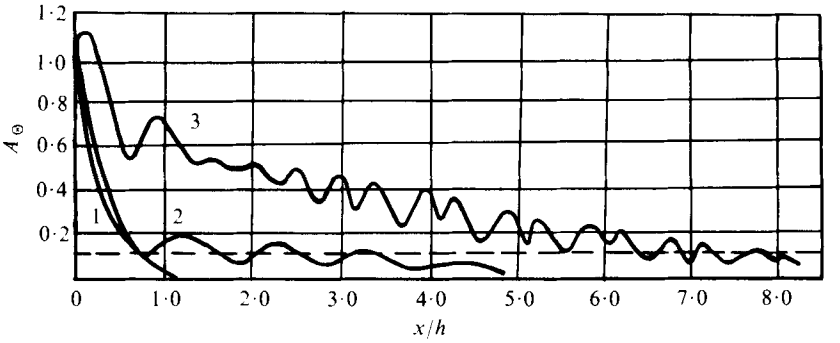

FIGURE 5. The shape of the TCW amplitude curve in a layer with rigid boundaries. $Pr = 1{\cdot}0$, $\omega = 0{\cdot}5$. (1) $\alpha = 0$, $Ra = 1500$. (2) $\alpha = \frac{2}{3}$, $Ra = 1500$. (3) $\alpha = \frac{2}{3}$, $Ra = 10^4$.

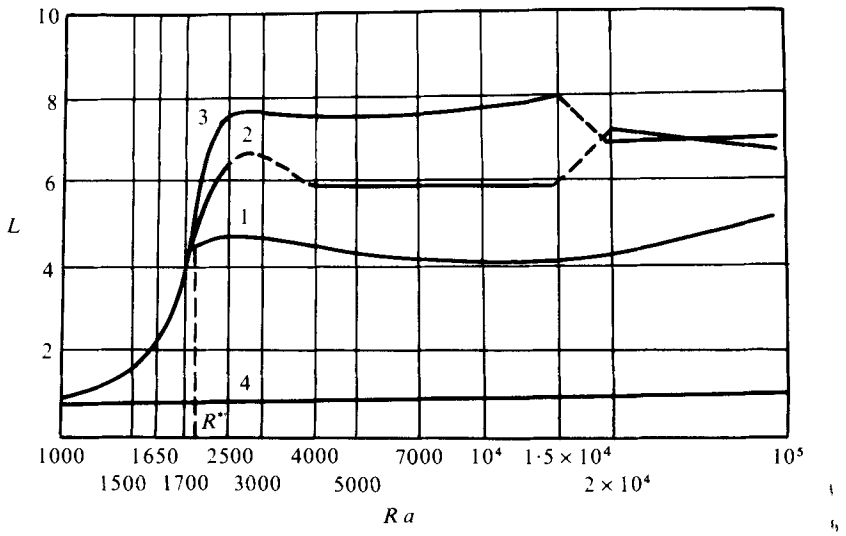

FIGURE 6. A plot of the damping length of TCW *vs.* the Rayleigh number. $\omega = 0{\cdot}5$. (1) $\alpha = 0{\cdot}8$. (2) $\alpha = 0{\cdot}5$. (3) $\alpha = \frac{2}{3}$. (4) $\alpha = 0$.

In an isothermal layer ($\alpha = 0$, $Ra = 0$) the temperature disturbances decay with distance x at a high rate (figures 5 and 6). It has been established that for the frequency range under consideration the effect of Gr on the propagation of temperature disturbances is significant only for $Gr > 2500$. At $Gr < 2500$ the propagation of temperature waves through a fluid is virtually the same as for a solid material as predicted by the linear theory. An analysis of the amplitude curve A_Θ for $Gr \geqslant 2500$ has demonstrated that near a vertical boundary where temperature modulation occurs temperature disturbances are damped at a higher rate compared with a solid material.

For a layer with a negative vertical temperature gradient, the propagation of disturbances is basically different: a number of peculiar alternating maxima and minima appear on the amplitude curve (figure 5) and the damping length is noticeably larger (figures 6 and 7).

The character of TCW propagation in the subcritical Rayleigh number range appears to be in good agreement with linear theory [see (16)]. The influence of a finite amplitude manifests itself in the fact that, as it increases, a greater portion of the

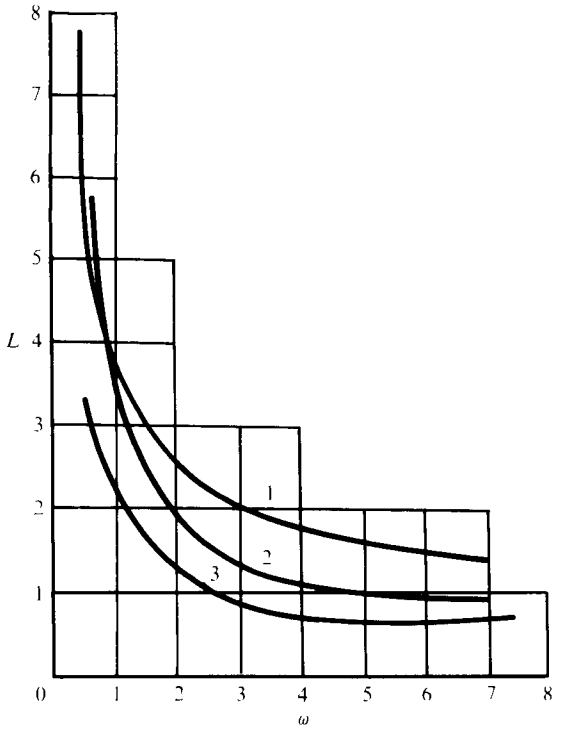

FIGURE 7. A plot of the damping length of TCW *vs.* the frequency. $\alpha = \frac{2}{3}$. (1) $Ra = 10^4$. (2) $Ra = 2500$. (3) $Ra = 1700$.

energy is spent on a strongly damped harmonic and nonlinear effects are exhibited near a vertical boundary.

In the supercritical range $Ra \geqslant R^*$ an appreciable increase in the oscillation amplitude along the layer is observed (figure 5). The disturbances propagate against the background of developed periodic convection owing to displacement of convective cells or to changes in their rate of rotation. A set of convective cells possesses a kind of 'elasticity', i.e. there is a restoring force which causes the disturbance to be transferred along the layer in the form of a wave. Three regimes of wave generation are possible, depending on the amplitude and frequency of the oscillations excited.

(*a*) In regime 1 an additional cell is periodically formed at the vertical boundary $x = 0$ and results in a region of compressed cells propagating along the layer.

(*b*) In regime 2 retardation and disappearance of the boundary cell lead to a region of expanded cells.

(*c*) In regime 3 a wave is generated without additional formation or disappearance of a boundary cell owing to periodic changes in the rate of convective motion.

The damping length of TCW depends essentially on which regime occurs. Regime 2 is most effective; regime 3 has the lowest efficiency. The bends in the curves in figure 6 may be explained by changes in the mechanism of TCW propagation. The damping length increases considerably with the Rayleigh number near the stability boundary. In the supercritical range L is strongly dependent on the frequency (figure 7). The damping length becomes significantly smaller as the Prandtl number increases (figure 8). The wavelength λ in the supercritical range depends on the distance between

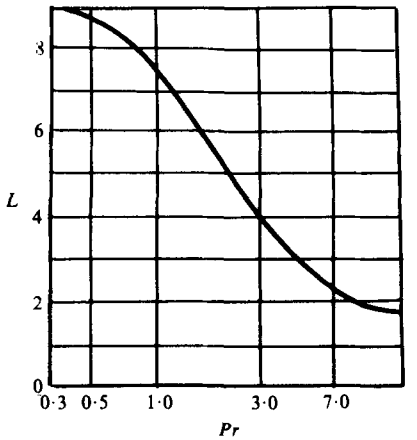

FIGURE 8. A plot of the damping length of TCW *vs.* the Prandtl number. $\alpha = \frac{2}{3}$, $Ra = 10^4$, $\omega = 0{\cdot}5$.

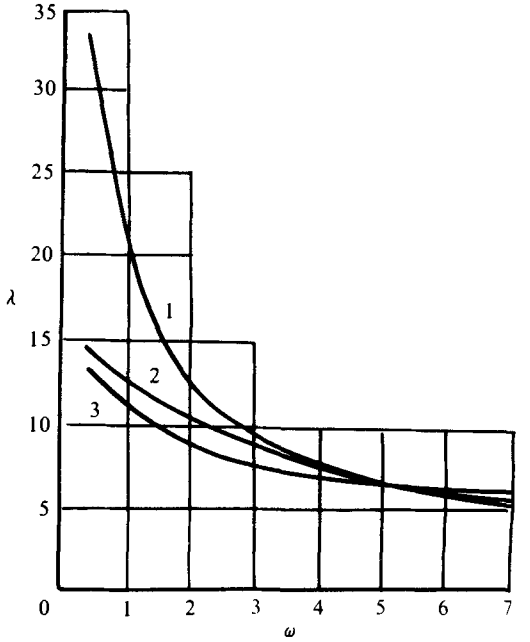

FIGURE 9. A plot of the TCW wavelength *vs.* the frequency. $\alpha = \frac{2}{3}$. (1) $Ra = 1700$. (2) $Ra = 2500$. (3) $Ra = 10^4$.

the centres of the neighbouring regions of compressed or expanded cells. For $Ra \geqslant 2500$ it depends on the frequency ω only slightly (figure 9).

The propagation of thermoconvective disturbances with finite amplitudes has been studied experimentally in the laboratory. The experimental set-up is described in the following section.

5. Experimental set-up

The experiments were carried out on a horizontal layer ($150 \times 50 \times 10{\cdot}2$ mm) of air ($Pr \sim 1$) uniformly heated from below and bounded by rigid walls ($l/h = 14{\cdot}7$). A copper plate with a nichrome heater constituted the lower boundary of the layer. The upper boundary was a heat exchanger consisting of glued Plexiglas sheets with water of controlled temperature circulating between them. The temperature behaviour was studied over the range $0 \leqslant Ra \leqslant 10^4$.

Periodic temperature oscillations at one of the vertical boundaries were produced by water which passed through a thermostat and was then pumped through a copper pipe of diameter 5 mm glued into the short side wall. The temperature variations of the water in the thermostat followed a certain law that determined the temperature behaviour of the vertical boundary. For periodic modulation of the temperature the electric heater of the thermostat was fed through a relay controlled by the signals from two contact thermometers installed in the thermostat and set for extremum temperature variations. The flow rate of water through the cooling coil of the thermostat was thereby maintained constant with the aid of a special unit. In this way the temperature modulation at the vertical boundary was kept close to a sinusoidal modulation with a circular frequency $\omega = 6 \times 10^{-1}$ to 6×10^{-3}(10^{-1} to 10^{-3} rad/s).

The temperature modulation was maintained at the mean temperature level in the layer for each temperature regime, which was controlled within an accuracy of $\pm 0{\cdot}1$ °C.

The system of temperature measurements involved (*a*) measuring the temperatures of the horizontal boundaries, (*b*) recording the modulating temperature at the side wall and (*c*) recording the temperature oscillations within the layer. The temperature distributions over the horizontal boundaries of the layer were measured by 24 copper–constantan thermocouples, the diameter of the wires being 0·1 mm. In all the runs deviations from the mean temperature of the wall were within 2 %. The temperature modulations at the vertical boundary were measured by five copper–constantan thermocouples uniformly glued over the wall height. A comb of three copper–constantan thermocouples with wire diameter 0·05 mm was used to register local temperatures in the layer. The comb was moved by a micrometer screw. The thermocouple readings were recorded on a multi-point potentiometer, which simultaneously measured the modulated temperature of the vertical boundary.

Visualization and photography of the structure of the convective motion were performed through the upper transparent heat exchanger. The convective structures were visualized with the aid of aerosol particles (tobacco smoke), which produced a clear flow pattern when illuminated by a helium–neon laser. Employing a special electromagnetic device, the beam was scanned over the width of the cavity with a frequency of 50 Hz at any horizontal section of the layer.

6. Discussion of the results and comparison with the predictions

Consider the propagation of temperature oscillations under isothermal conditions (with the horizontal boundaries of the layer maintained at the same temperature). As shown by the amplitude curves (figure 10), the amplitude of the temperature oscillations over a half-height of the layer decreases rapidly as the distance from the

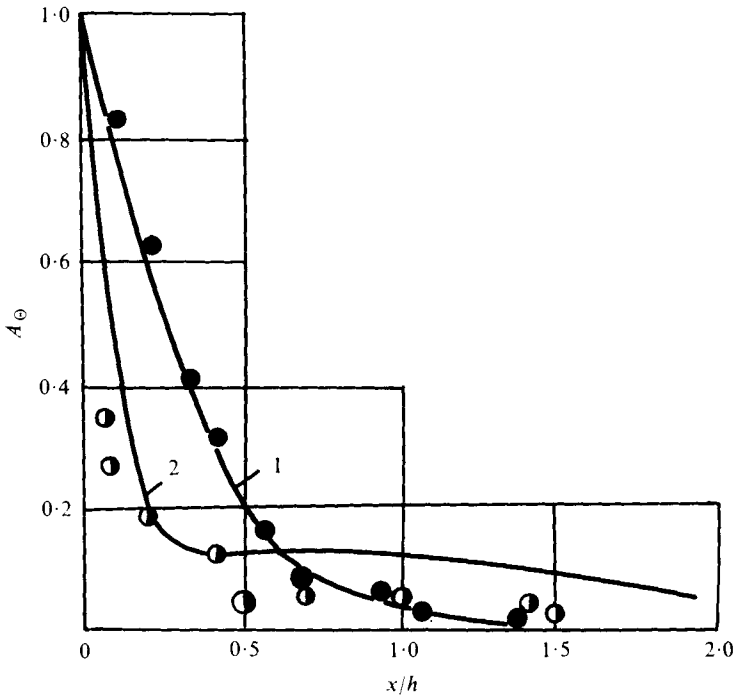

FIGURE 10. Attenuation of temperature oscillations under isothermal conditions. (1) $A_\Theta = \exp(-\pi h^{-1}x)$. (2) $A_0 = 15$ °C, $\omega = 0{\cdot}2$. ●, $A_0 = 15$ °C, $\omega = 0{\cdot}2$; ◑, $A_0 = 15$ °C, $\omega = 0{\cdot}2$.

vertical boundary with modulated temperature increases. For a frequency of temperature oscillations $\omega \geqslant 10^{-1}$, the temperature oscillations along the layer are damped in the same manner as in a solid of height $h = 10{\cdot}2$ mm (ordinary temperature waves). In this case the decrease in the amplitude of the temperature wave along the solid is described by the expression $A_\Theta = \exp(-\pi h^{-1}x)$ (curve 1). Because of the lower frequency of the temperature modulation, curve 2 (the amplitude curve obtained numerically) departs from curve 1. When the temperature distribution at the vertical boundary is not linear, convective motion arises naturally. For a high frequency modulation the rate of convective motion appears to be so small that the motion has no effect on the propagation of temperature oscillations, which therefore travel in the same manner as in a solid under isothermal conditions.

As the frequency of the temperature oscillations decreases, the convective motion at the vertical boundary becomes periodic in time, the rotation of a convective cell continually changing its direction with a period equal to that of the temperature oscillations at the vertical boundary. Sharper attenuation of temperature oscillations near the vertical boundary is caused by heat transfer from the side wall to the horizontal boundaries of the layer.

Propagation of disturbances in a non-isothermal layer with a vertical temperature gradient at $Ra < 1200$ follows the same pattern as that at isothermal conditions.

As the Rayleigh number increases in the subcritical range, the amplitude curve exhibits a number of alternating maxima and minima associated with the convective structures due to the temperature disturbances (figure 11). The number of peaks in the

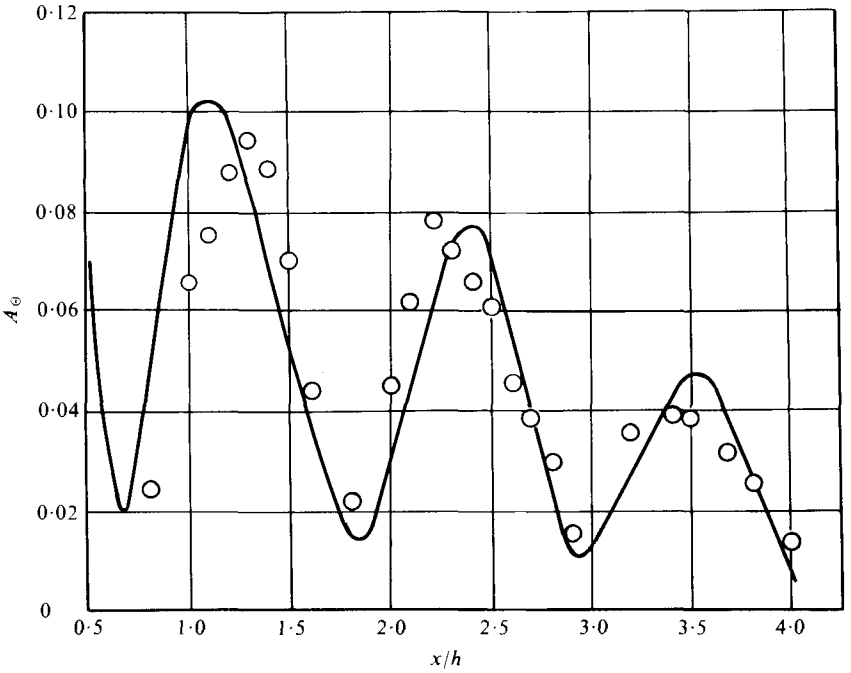

FIGURE 11. The shape of the TCW amplitude curve in the subcritical range. ——, $Ra = 1500$; ○, $Ra = 1660$.

amplitude curve depends on the vertical temperature gradient. The solid line in the figure shows the numerical results; experimental data are represented by circles.

The structure of the convective motion in the layer under supercritical heating controls the propagation of temperature disturbances from the wall. When the vertical temperature drop has reached its critical value for the present layer height, steady-state convection exists in the layer in the form of hexagonal cells which are stable at Rayleigh numbers not exceeding $Ra \simeq 2500$ (figure 12*a*, plate 1). In the region with $Ra = 2500$ elongation of the cells in the transverse direction is observed (figure 12*b*, plate 1). With a further increase in the temperature drop rolls with axes parallel to the short side boundary of the layer are formed. Such a structure appeared to be stable in the range of supercritical Rayleigh numbers studied and to be preferred in narrow rectangular layers (Davis 1967). This transition from cellular to roll-like convection has been predicted theoretically for an infinite horizontal layer by Palm, Ellingsen & Gjevik (1967) and obtained experimentally for a layer with finite dimensions by Koschmieder (1966). Generation of temperature disturbances at a side boundary leads to a periodic variation in the structure of the convective motion. In one half of each period an additional convective roll is formed near the side boundary with modulated temperature and the region of compressed rolls propagates along the layer. In the next half-period of the temperature modulations the former convective structure is restored. Thus transmission of temperature disturbances is carried out by displacement of convective structures through generation of an additional roll. This corresponds to regime 1 of the generation of a thermoconvective wave observed in the numerical experiments. The temperature amplitudes at all points of the layer increase con-

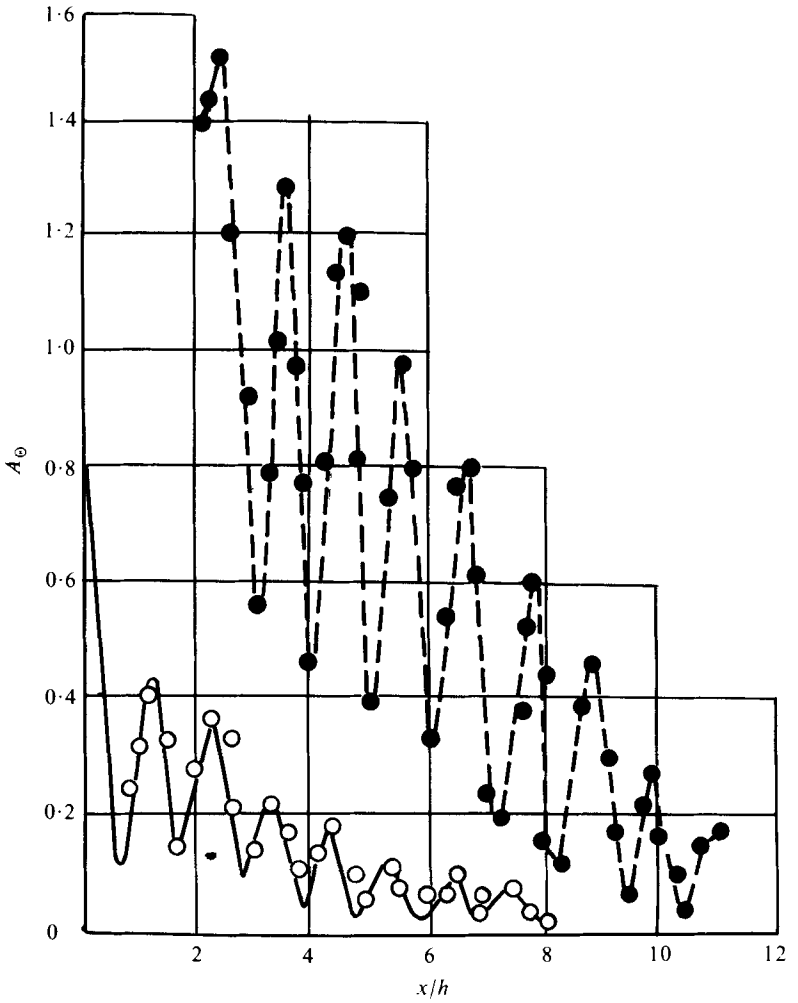

FIGURE 13. Amplitude curves of TCW in the supercritical range.
—, $Ra = 1500$; ○, $Ra = 1660$.

siderably with distance (figure 13). The solid line in this figure shows the numerical results. It is probably because a coarse net was used in the calculations ($\Delta x = \frac{1}{15}$), which results in a considerable error, that the numerical ($\omega = 0{\cdot}45$) and experimental ($\omega = 0{\cdot}18$) results coincide. The broken line connects experimental points for $Ra = 3400$ and $\omega = 0{\cdot}012$. The characteristics of TCW in the supercritical range are determined by the frequency of the temperature oscillation rather than by the Rayleigh number. As has been demonstrated experimentally, at sufficiently low frequencies at the vertical boundary ($\omega \sim 10^{-2}$) intensification of the temperature oscillations is possible: the amplitudes of the temperature oscillations in the layer exceed those at the vertical boundary.

The thermoconvective wavelength is determined experimentally from the phase shift between the temperature oscillations in the layer and at the vertical boundary. In the subcritical range the wavelength is found to be ~ 30–$70h$ and inversely proportional to a frequency of the temperature oscillations. It is evident that in this

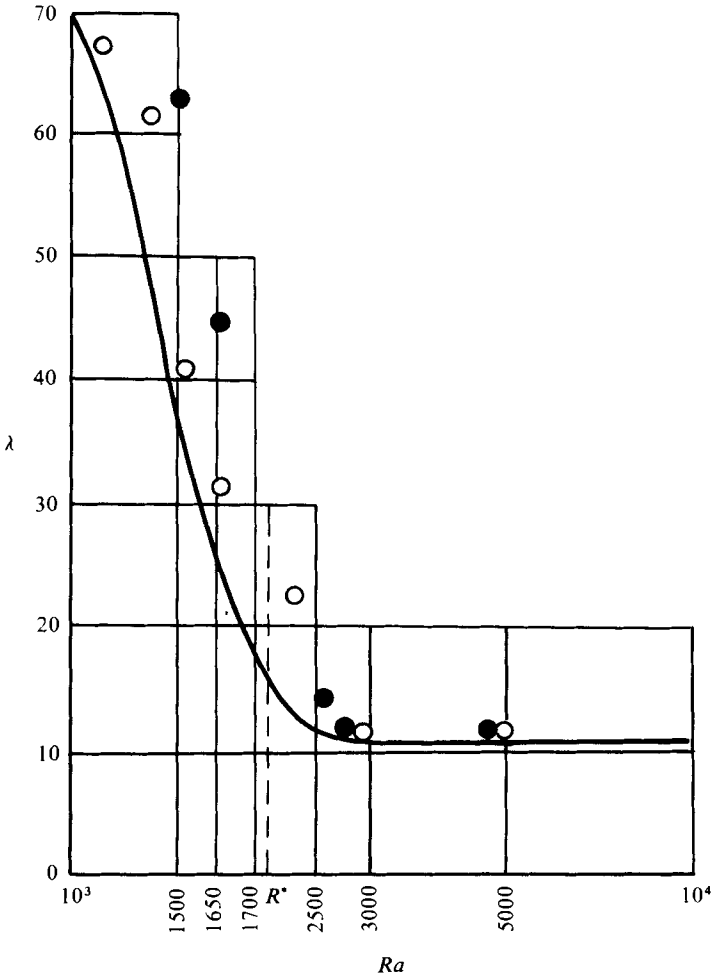

FIGURE 14. A plot of the TCW wavelength *vs.* the Rayleigh number. ——, numerical calculation; ○, $\omega = 0{\cdot}45$; ●, $\omega = 6 \times 10^{-2}$.

situation the phase velocity is independent of the frequency of the temperature oscillations over the range investigated. At the same time the rate of the thermoconvective wave propagation depends essentially on the vertical temperature drop in the layer and decreases as this grows. In the subcritical range the rate of propagation of TCW is $\sim 2 \times 10^{-3}$ to 8×10^{-3} m/s.

Figure 14 is a plot of the TCW wavelength λ *vs.* the Rayleigh number. The numerical results for $\omega = 0{\cdot}5$ are depicted as a solid curve. The weak dependence of λ on the Rayleigh number for $Ra > 2500$ is verified experimentally.

The damping factor Im K determines the decrease in the TCW amplitude along the layer. A plot of Im K *vs.* the Rayleigh number is presented in figure 15. The solid line represents the numerical results. Experimental data are shown as circles. A sharp decrease in TCW damping at the critical Rayleigh number may be seen clearly.

It should be emphasized that in the supercritical range dispersion has been observed. The propagation of thermoconvective disturbances should therefore be characterized by a group velocity of 10^{-3}–10^{-2} m/s.

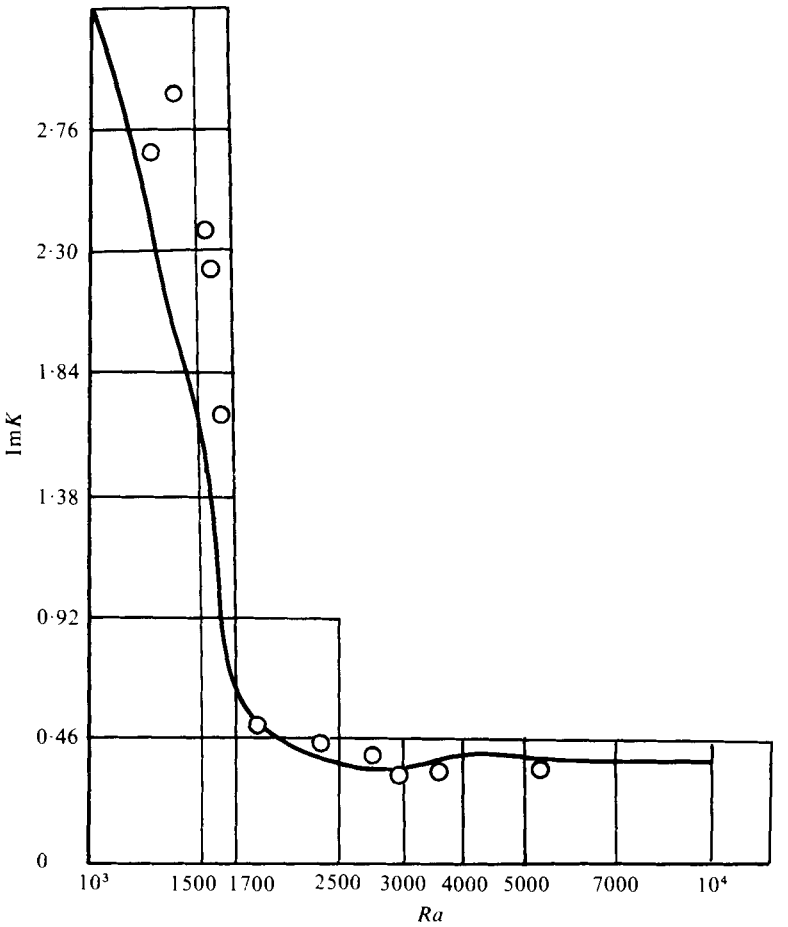

FIGURE 15. A plot of the damping factor *vs.* the Rayleigh number.

Figure 16 shows simultaneous records of the temperature modulation at the half-height of the side boundary and the temperature oscillations in the layer. At the system exit (the air layer being heated from below) a signal is sent in a form close to triangular. In the layer a temperature change close to harmonic is registered. A Fourier analysis of the temperature oscillations has shown that the spectral composition of a temperature signal changes as it propagates along the layer. The amplitudes of the higher harmonics of the exit signal, which are initially $3\omega \sim 0{\cdot}1A_0$ and $5\omega \sim 0{\cdot}05A_0$, decrease considerably with distance from the side boundary. Thus, for the signal at a point $x/h = 4{\cdot}6$, the amplitude of the harmonic 3ω equals approximately $0{\cdot}03A_0$ and that of the harmonic 5ω approximately $0{\cdot}01A_0$. It is natural that with decreasing frequency the damping length of thermoconvective waves increases and the damping decrement decreases.

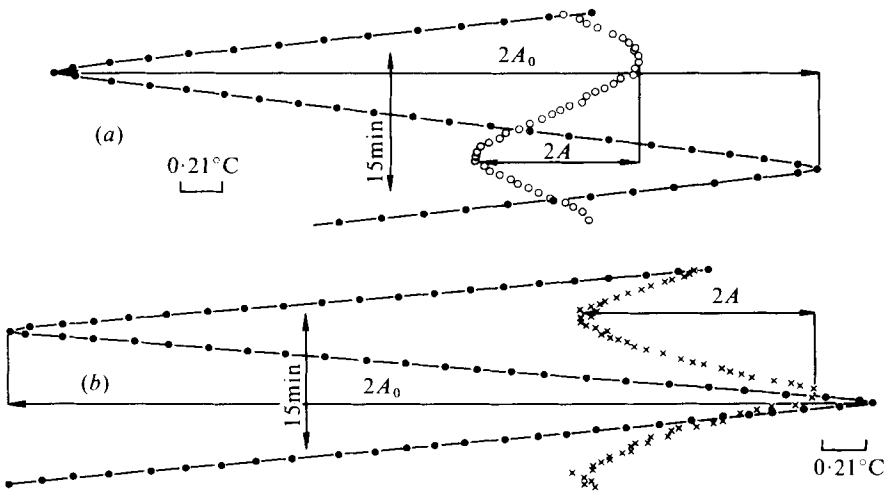

FIGURE 16. Simultaneous temperature records. ●, at the side boundary; ○, ×, in the layer. (*a*) $x = 4{\cdot}6$. (*b*) $x = 6{\cdot}8$.

7. Conclusions

A general investigation has been made of a particular mechanism of wave propagation of interrelated thermal and hydrodynamic disturbances in horizontal unstably stratified layers of viscous heat-conducting fluid. A thorough investigation of this mechanism appears to be of interest from both the theoretical and the experimental point of view.

It seems reasonable that further investigations of TCW should study:

(*a*) TCW propagating near the threshold of oscillatory instability of convective motion;

(*b*) TCW with combined forced and natural convection;

(*c*) TCW in fluids with peculiar properties, particularly electrically conducting and ferromagnetic fluids.

REFERENCES

BARKOV, YU. I., BERKOVSKY, B. M. & FERTMAN, V. E. 1974 *Inzh.-Fiz. Zh.* **27**, 618.

BERKOVSKY, B. M., BASHTOVOI, V. G. & LIPKINA, E. A. 1970 Thermoconvective waves in conducting and ferromagnetic fluids. *Energy Transfer in Ducts*, p. 39. Minsk: Nauka i Tekhnika.

CARSLAW, H. S. & JAEGER, J. 1959 *Heat Conduction in Solids*. Oxford: Clarendon Press.

CHANDRASEKHAR, S. 1961 *Hydrodynamic and Hydromagnetic Stability*. Oxford: Clarendon Press.

DAVIS, S. H. 1967 *J. Fluid Mech.* **30**, 465.

DRAZIN, P. G. 1975 *Z. angew. Math. Phys.* **26**, 239.

GERSHUNI, G. Z. & ZHUKHOVITSKY, E. M. 1972 *Convective Stability of Incompressible Fluids*. Moscow: Nauka.

GITERMAN, M. SH. & SHTEINBERG, V. A. 1972 *Izv. Akad. Nauk SSSR, Mekh. Zh. i Gaza* **2**, 55.

GOLITSIN, G. S. 1965 *Izv. Akad. Nauk SSSR, Fiz. Atmos. i Okeana* **1**, 136.

GUPTA, P. S. & GUPTA, A. S. 1973 *Japan J. Appl. Phys.* **12**, 1881.

KOSCHMIEDER, E. L. 1966 *Beitr. Phys. Atmos.* **39**, 1.

LEBLOND, P. H. 1966 *J. Fluid Mech.* **25**, 121.

LUIKOV, A. V. & BERKOVSKY, B. M. 1969*a* *Dokl. Akad. Nauk LBSSR* **13**, 316.

LUIKOV, A. V. & BERKOVSKY, B. M. 1969*b* *Inzh-Fiz. Zh.* **16**, 780.

LUIKOV, A. V. & BERKOVSKY, B. M. 1970 *Int. J. Heat Mass Transfer* **13**, 741.

NOGOTOV, E. F. & SINITSYN, A. K. 1975 Numerical investigation of thermoconvective waves in ferromagnetic fluid layers. *Investigation of Convective and Wave Processes in Ferromagnetic Fluids*, p. 3. Minks: ITMO Akad. Nauk BSSR.

PALM, E., ELLINGSEN, T. & GJEVIK, B. 1967 *J. Fluid Mech.* **30**, 651.

SINITSYN, A. K. & FERTMAN, V. E. 1976 *Izv. Akad. Nauk SSSR, Fiz. Atmos. i Okeana* **10**, 1115.

TAKASHIMA, M. 1972*a* *Phys. Lett.* A **38**, 75.

TAKASHIMA, M. 1972*b* *J. Phys. Soc. Japan* **33**, 1712.

THOMAS, N. H. & STEVENSON, T. H. 1973 *J. Fluid Mech.* **61**, 301.

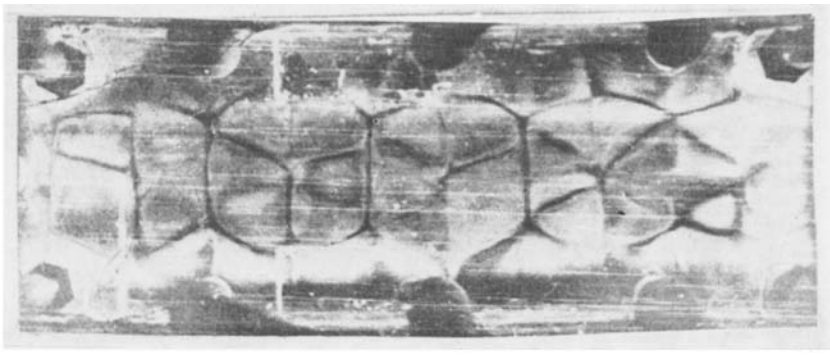

(*a*)

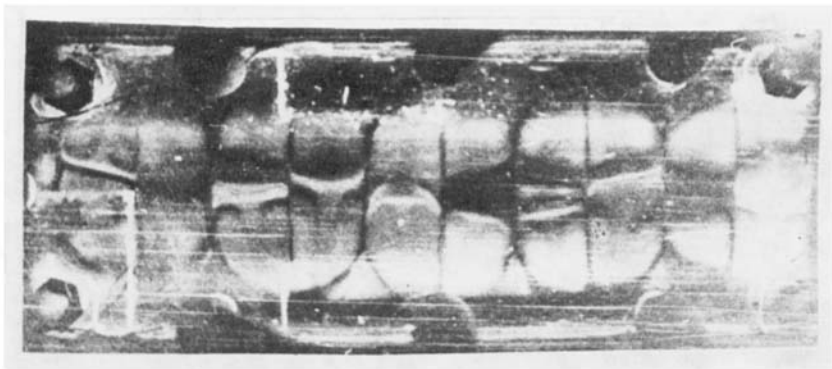

(*b*)

(*c*)

FIGURE 12. Variation of structure of convective motion in a cavity with increasing Rayleigh number.